RSC Advances

PAPER

View Article Online
View Journal | View Issue

Cite this: *RSC Adv.*, 2021, **11**, 20507

A millifluidic chip for cultivation of fish embryos and toxicity testing fabricated by 3D printing technology†

Petr Panuška,[a] Zuzana Nejedlá,[a] Jiří Smejkal,[a] Petr Aubrecht,[a] Michaela Liegertová,[a] Marcel Štofik, *[a] Jaromír Havlica[bc] and Jan Malý [a]

Zebrafish (*Danio rerio*) serves as a popular animal model for *in vivo* acute toxicity evaluation with the Fish embryo test (FET). Over the last few years there has been an effort to develop various systems for a high-throughput zebrafish embryo cultivation and FET. In this paper, we present a novel design of a millifluidic system fabricated by 3D printing technology and we evaluate its functional properties on *Danio rerio* embryos cultivation and toxicity testing. The development and the optimization of the millifluidic chip was performed by experimental measurements supported by numerical simulations of mass and momentum transport. The cultivation chip with two inlets and one outlet consisted of two individual channels placed on top of each other and separated by a partition with cultivation chambers. An individual embryo removal functionality, which can be used during the cultivation experiments for selective unloading of any of the cultivated embryos out of the chip, was added to the chip design. This unique property raises the possibility of detailed studies of the selected embryos by additional methods. Long-term (96 hours) perfusion cultivation experiments showed a normal development of zebrafish embryos in the chip. Model toxicity tests were further performed with diluted ethanol as a teratogen. Compared to the FET assays, an increased toxic effect of the ethanol on the embryos cultivated in the chip was observed when the median lethal dose and the percentage of the morphological end-points were evaluated. We conclude that the presented 3D printed chip is suitable for long-term zebrafish embryo cultivations and toxicity testing and can be further developed for the automated assays.

Received 31st January 2021
Accepted 25th May 2021

DOI: 10.1039/d1ra00846c

rsc.li/rsc-advances

1. Introduction

In the last few decades, zebrafish (*Danio rerio*) has been established as a suitable animal model for toxicity testing by acute toxicity tests, the so-called fish embryo tests (FETs).[1] It has also been widely used in genetics and developmental biology,[2,3] in different toxicological studies,[4] for drug screening,[5] drug discovery,[6] and ecotoxicology.[7] A typical experimental procedure for fish embryo toxicity testing is realized in multiwell plates. This option has also been used in commercially available testing procedures.[8] However, the major drawback of using multiwell plates is a time-consuming manual operation by the experimenter, which could be automized for high-throughput testing. Microfluidics has been referred to as a competitor to the traditional multiwell plates-based tools[9–11] and has been employed in invertebrates and vertebrates experimental studies.[12] Moreover, commercial microfluidic products for zebrafish experiments are available.[13]

Microfluidics for zebrafish, also called fish-on-a-chip technology,[14] can be designed for embryonic[15,16] and larval zebrafish studies.[17] Microfluidic channels for embryonic studies (the embryo is enclosed inside the embryonic envelope – chorion) have larger dimensions compared to microfluidics systems designed for zebrafish larvae (zebrafish developmental stage after hatching with a similar body shape to adult fish). Microfluidic chips adjusted to embryos can manipulate and treat the embryos as small rigid spherical objects (fish eggs). Chips usually include immobilization chambers. They are designed for long-term experiments, but the experiments are limited by the time of the embryo hatching. The hatching time can range from 48 to 72 hours post-fertilization (hpf) depending on the temperature.[18] Such microfluidic chips enabled to perform various perfusion experiments.

Up to now, several toxicity studies of various chemicals performed in perfusion systems with the fish-on-a-chip technology have been presented. As an example, Lamer *et al.*[19] modified commercial polystyrene microtiter plates to be used

[a]*Department of Biology, Faculty of Science, University of J.E. Purkyne, 400 96 Usti nad Labem, Czech Republic. E-mail: marcel.stofik@ujep.cz; Tel: +420 475 283 376*

[b]*Department of Chemistry, Faculty of Science, University of J.E. Purkyne, 400 96 Usti nad Labem, Czech Republic*

[c]*Czech Academy of Sciences, Institute of Chemical Process Fundamentals, Rozvojova 2/135, 165 02 Prague, Czech Republic*

† Electronic supplementary information (ESI) available. See DOI: 10.1039/d1ra00846c

for flow-through cultivations. Although their system was not a microfluidic chip, they tested the toxic effects of 4-chlorophenol under continuous perfusion and compared EC50 values with a standard static FET, yielding a slightly higher toxicity under the perfusion conditions. Ethanol toxicity in microfluidic perfusion system was evaluated by Wielhouwer *et al.*[20] Yang *et al.*[21] developed a microfluidic system with an integrated concentration gradient generator (CGG) and open cultivation chambers to test the toxicity and the teratogenicity of doxorubicin, 5-fluorouracil and cisplatin. Similar microsystem architecture was used by Li *et al.* They included CGG in the system with closed cultivation chambers for zebrafish embryos perfusion experiments to study the toxicity and the teratogenicity of aminophylline[22] and the toxicity of lead and copper.[23] Choudhury *et al.*[24] examined the toxic effects of valproic acid and Akagi *et al.*[25] studied the angiogenesis inhibition effect of anti-angiogenic drugs in 3D multilayer chip-based system. The toxicity of copper sulphate pentahydrate was tested under the perfusion conditions in microfluidic FET (μFET) and compared to static FET experiments by Zhu *et al.*[26] They evaluated higher LC50 value in perfusion conditions. They also tested four reference organic toxicants – DMSO, ethanol, caffeine, and phenol, using the μFET protocol. The results showed similar toxicity for the perfusion and the static conditions, with slightly higher EC50 values for DMSO in the perfusion and for phenol and caffeine in the static conditions. A less stable compound (nicotine) has also been tested. It showed significantly (around 40%) lower EC50 value for the perfusion conditions, pointing out a potential advantage of the microfluidic approach in better control of the cultivation conditions (more stable concentrations of less stable substances).

The current microfluidics benefits from the use of polymers as building materials mainly due to their low costs and simplified manufacturing procedures.[27] The most published techniques employed for the zebrafish embryo cultivation system are techniques using PDMS, where the master was manufactured by laser cutting[23,25] or by 3D printing.[28] Also, individual PMMA sheets cut by a laser micromachining method can be layered and assembled by thermal bonding to create a suitable cultivation microenvironment.[26,29] The layering technique can also be used for the fabrication of a borosilicate-glass cultivation chip,[20] but glass structuring is not easy and expensive equipment is needed. All the described techniques require several fabrication steps to manufacture the whole system. Recently, 3D additive manufacturing (AM) has become an alternative processing technique in microfluidics.[30,31] The advantage of 3D AM is the possibility to quickly design the required structures of the system parts by a broadly available computer-aided design (CAD) software and to transfer the created models directly to the fabrication process to produce complex structures in 3-dimensional space by cheap and rapid manufacturing. 3D AM has also been proved as a possible technology for fabrication of zebrafish cultivating systems.[15] Such systems can be referred to as millifluidic, due to larger critical dimensions, and particularly when they are manufactured by 3D printing.[32]

Despite many advantages of the fish-on-a-chip technology presented so far, one of the main drawbacks is the impossibility of selective manipulation with an individual embryo immobilized in the system and the non-uniform medium flow over all the embryos in the system.[20,21,28] It is common that even in the control group, some of the embryos naturally fail to develop and coagulate in the early stages of the development. For the FET to be valid, the overall survival of the embryos in the negative control should be ≥90% by the 96 hours exposure (up to 10% embryo mortality is tolerated).[1] Therefore, it would be favorable for the system to have a functionality enabling a depletion of dead embryos during each stage of the cultivation experiment to prevent the negative influence of the decaying processes on the downstream embryos in the system. It could also be useful to be able to perform additional individual embryo analysis out of the perfusion system at a certain stage of its development. Moreover, the system should ideally be designed in such a way that the medium flows equally around all the embryos and uniformly all over the surface of the individual embryo.

This work presents a new design of a millifluidic cultivation chip for zebrafish embryos reflecting the important requirements mentioned above. The chip consists of top and bottom channels enabling the uniform media perfusion around the embryos along the whole chip. The channels are divided by a partition with 24 holes for the immobilization of the embryos. The chip is fabricated by a 3D printing digital light processing (DLP) technology, and if necessary, the cultivation part can be further expanded. The chip has an extra individual embryo removal functionality, which has been tested with a 3D-printed manual and automated 24-port selection switch valve actuated by a stepper motor controlled by the Arduino microprocessor. We show full functionality of the developed chip in long-term embryo cultivation and we present model toxicity studies. Our system can be used as a cheap semi-automated middle-throughput perfusion system and as an alternative to expensive robotic systems with an individual embryo removal functionality. To our best knowledge, the presented microchannels design of the chip and the embryo removal system for zebrafish cultivation have not been published yet.

2. Materials and methods

2.1. Chemicals and material

E3 medium (embryo cultivation medium) was freshly prepared prior to use. It consisted of deionized water, 5 mM NaCl, 0.17 mM KCl, 0.33 mM $CaCl_2$ and 0.33 mM $MgSO_4$. The salts for the medium preparation and other chemicals such as 96% ethanol p.a., isopropanol p.a. and trypan blue were provided by Sigma-Aldrich s.r.o., Czech Republic. Other material used for the experiments was: 1.6 mm ID silicone tubing (ibidi GmbH, Germany), 1/16″ OD × 1/32″ ID PTFE tubing (Darwin Microfluidics, France), 1/8″ OD × 0.062″ ID PFA high purity tubing, 1/4–28 fittings with ferules and manual shut-off valves, debubblers and solvent caps for 1/4–28 fittings, all provided by Cole-Parmer Instrument Company Ltd, Great Britain. For the FET cultivation experiments, 96-well microtiter plates (Sigma-Aldrich s.r.o., Czech Republic.) and a home-made thermobox

with Arduino-based PID temperature control (incubator) were used.

2.2. Design and fabrication of the cultivation system

The design of the chip and all the added components was developed by using Autodesk Fusion 360 (Autodesk, Inc., USA) CAD software. For the fabrication, 3D printing and CNC milling technology were used. The 3D printing was performed with a digital light processing (DLP) Perfactory® IV LED printer (Envisiontec GmbH, Germany) with a build envelope size of 84.08 × 52.58 mm, layer thickness 100 μm and resolution 1920 × 1200 px (resulting native pixel size 44 μm) and FDM Original Prusa i3 MK3S ED printer (Prusa Research a.s., Czech Republic). The CNC milling fabrication of the designed parts was provided by a local company (Denas Děčín spol.s r.o., Czech Republic). The cultivation system included several individual parts: (i) a chip, (ii) a system for a single embryo removal, (iii) a chip holder with temperature control. The system for a single embryo removal (microchannels) as a part of the chip and the 3D printed 24-switch valve used for the embryo removal system were designed and tested as a proof-of-concept. For more details on the 3D printed 24-switch valves and on the chip holder with temperature control, see ESI.†

The millifluidic chip was fabricated as a 2-component system. The whole body of the chip was printed from E-Shell 300, photo-reactive acrylate (Envisiontec GmbH, Germany), on a DLP 3D printer. The bottom transparent part was made from polymeric foil (supplied by a local store) laminated to the bottom part of the chip through biocompatible adhesive tape (~142 μm thick double-sided adhesive tape ARcare 90106NB, provided by Adhesives Research Ireland Ltd., Ireland). First, the chip body was printed. The adhesive tape was cut with a laser cutter (provided by a local company Karel HAINZ, Czech Republic). The shape of the cut openings corresponded to the bottom channels of the chip body. The adhesive tape and then the foil were manually laminated to the bottom part of the chip. The chip body also included eight holes with M3 threads for fixation of the chip interface module. The details of the chip are presented in Fig. 1.

Every chip was treated by standard hardening and leaching procedure prior to use. After the printing, every chip was rinsed in two subsequent isopropanol sonication baths, each two

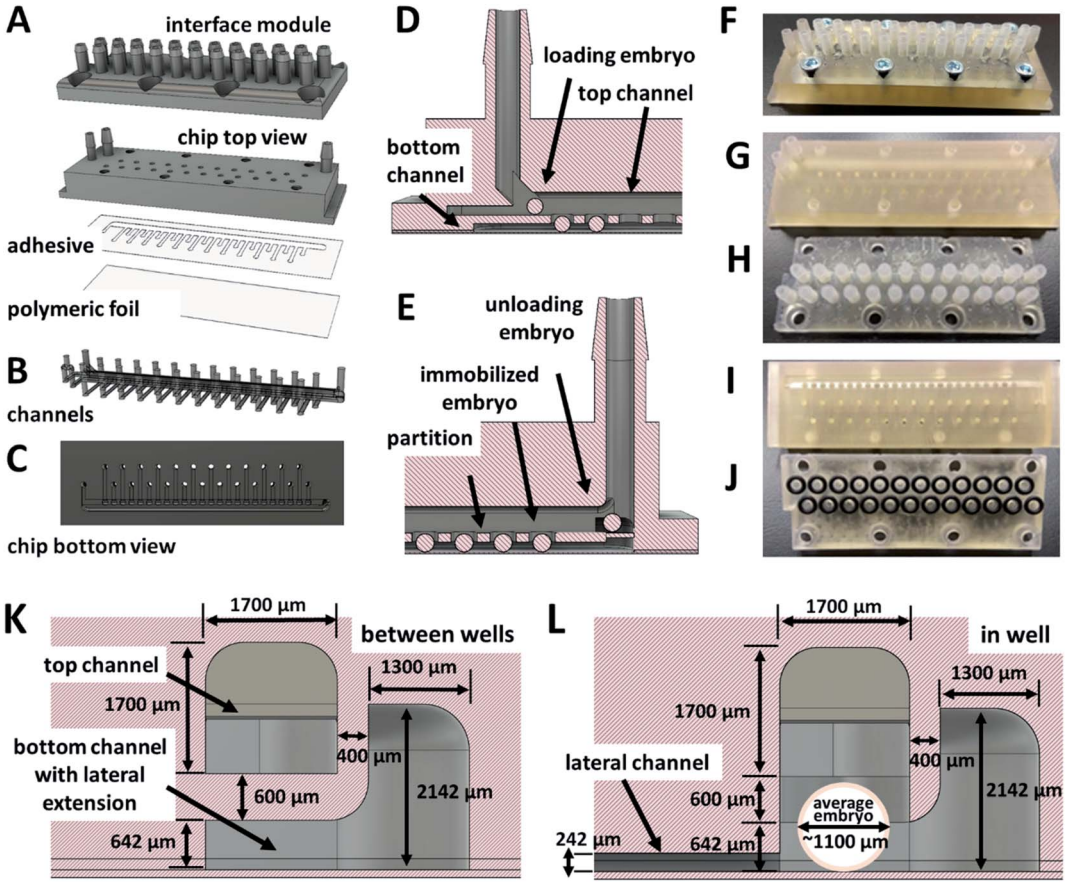

Fig. 1 A millifluidic chip for the cultivation of *Danio rerio* embryos. (A) An exploded view of the cultivation chip components. From the top: (i) an interface module for the connection of the system for a single embryo removal, (ii) the chip body (from a top-side view), (iii) the adhesive, and (iv) transparent polymeric foil; (B) the channels of the chips; (C) a bottom view of the chip; (D) and (E) a side cut view of the front and the rear parts of the chip, respectively. (F–J) 3D-Printed parts of the cultivation chip: (F) the chip with an interface module, (G) the chip alone, (H) the interface module alone, (I) a bottom view of the chip, and (J) a bottom view of the interface module, including o-rings. (K) and (L) front cut views between and in the center of a cultivation well.

minutes long. The chips were dried by a nitrogen flow and the top and the bottom side were exposed to a 550 W mercury light source of a manual photolithograph (Newport Corporation, USA), one hour each side. Then, the chips were leached in two subsequent 96% ethanol baths, each for 24 hours. In the next step, the chips were thoroughly washed in distilled water and were dried by nitrogen flow. Before the experiments, the chips were primed by an E3 medium at a flow rate of 80 μl min^{-1} for 24 hours.

2.3. Numerical simulations

The main goal of the numerical simulations of the mass and momentum transport in the chip channels was to optimize the geometry of the device. The velocities and pressure fields were obtained by solving the continuity equation and the Navier–Stokes equations in steady-state for an incompressible fluid under isothermal conditions. In addition to the fluid flow, also the transport of toxicants using the convection–diffusion equation was solved. For discretization, the finite element method was used. The number of the elements of the non-uniform numerical grid ranged from 2.5×10^6 to 3.5×10^6. The variation of the number of the elements was dependent on the used geometry. A non-uniform grid had to be used to perform simulations on geometries with lots of internal obstructions.

The following boundary conditions were used for: (i) inlet – constant velocity in the normal direction to the inlet plane, zero derivation of pressure in the normal direction and constant concentration of toxicants; (ii) outlet – zero derivation of velocity in the normal direction, constant value of pressure and zero flux of toxicants concentration in the normal direction; (iii) walls and surface of eggs – no slip boundary condition and zero flux of toxicants concentration in the normal direction. Simulations were performed in Autodesk CFD software (Autodesk, Inc., USA).

2.4. Zebrafish maintenance

Fish adults of the wild type of *Danio rerio* were used as an experimental fish model for the testing. All adults were 1–2 years old and in good condition. They were kept in a photoperiod of 14L:10D (14 hours of light and 10 hours of darkness). Spawning of the embryos was done once or two times in a 14 day interval. One day before spawning, the zebrafish adults were transferred into individual plastic cages at the beginning of the dark photoperiod. The sex ratio was kept 3M:2F (three males and two females). All zebrafish were spawned at the end of the dark photoperiod. Fertilized eggs were collected within 30 minutes after fertilization and transferred to a clean E3 medium kept at 25.0 °C. Before use, the eggs were inspected with a stereomicroscope for health and the developmental stage.

2.5. Embryo cultivation experiments and toxicity assays

Three hours post-fertilization, the embryos were used for cultivation and toxicity testing. Prior to the load of the embryos into the chip, each embryo was carefully inspected, and if any developmental abnormality was observed, the embryo was discarded. Ethanol was used as a teratogenic toxicant in the model toxicity tests.

To evaluate the functionality of the chip, several cultivation experiments were performed under perfusion conditions. First, the embryos were manually loaded into the tubing by a medical syringe. The distance between the embryos in the tubing was 30 mm to prevent their close contact, which could result in sticking them together. The tubing with the embryos was connected to the loading port of the chip and the flow rate of the medium in the chip was set to 30 μl min^{-1}. The embryos were slowly loaded into the cultivation chambers of the chip by a slight pressure on the piston of the syringe. After the embryos were delivered to the cultivation chambers of the chip, the flow rate of the medium was set to 80 μl min^{-1} for one hour. Then the flow rate was decreased to 30 μl min^{-1}, and the cultivation experiment started. During the loading steps, the E3 medium was always used. In the toxicity experiments, the E3 medium was exchanged for toxicant (ethanol) one hour after the embryos were loaded, which corresponded to 4 hpf. The time of the cultivation was set to 96 hours. During the testing, images of each cultivation chamber were acquired in 15 minute intervals by an automatic algorithm programmed in cellSense software (Olympus Czech Group, s.r.o., Czech Republic). The time interval for the image acquisitions was set the same in all experiments performed with the chips. The media actuation was controlled with a pressure controller OB1 MK3+ and with MFS 3 flow sensors (all from ELVEFLOW, France) with the flow rate control range of 2–80 μl min^{-1}. The same conditions were kept during the toxicity tests.

The cultivation and toxicity assays in 96-well microtiter plates were performed as standardized *in vivo* FET bioassays according to OECD guidelines for testing of chemicals. For each toxicant concentration, 24 embryos were used, and every single embryo was considered as an individual replicate for the statistical analysis. All embryos were incubated and inspected in microtiter plate wells, filled with 200 μl of media, at a constant temperature of 25.0 °C for 96 hours. The solution with the toxicant was manually exchanged once, after 48 hours. The images of the inspected embryos were acquired at 24 hpf, 48 hpf, 72 hpf, and 96 hpf. In both assays types, the FET tests and the perfusion toxicity assays, the embryos were scored for mortality by evaluation of six morphological endpoints: (i) coagulation, (ii) lack of somite formation, (iii) growth retardation, (iv) malformation, (v) lack of the tail-bud detachment from the yolk sac, (vi) heart edema. Perfusion toxicity tests were designed to follow the FET testing. For each toxicant concentration, 24 embryos were loaded in the cultivation chip, and every single embryo was considered as an individual replicate. The flow rate of the toxicant was kept to 30 μl min^{-1}. The experiments were running at a constant temperature of 25.0 °C for 96 hours.

2.6. Data collection and evaluation

All image data of the embryos developmental stages were collected with an inverted optical microscope Olympus IX73 (Olympus Czech Group, s.r.o., Czech Republic) equipped with

an objective UPLFLN4X, a digital camera Olympus DP80 with dual CCD sensors, motorized stage SCAN IM for inverse microscopes (Märzhäuser Wetzlar GmbH & Co. KG, Germany) and pE-4000 illumination system (CoolLED Ltd., Great Britain). The image acquiring was programmed within cellSens Dimension Olympus software, so the image collection of the embryos immobilized in millifluidic chips was performed in an automated mode. The automated algorithms with a time-lapse image acquisition of each cultivation chamber at a 15 minute time interval were prepared in Experiment Manager of the cellSense software. The combination of the motorized microscope stage, the illumination system, and the time-lapse programs provided a fully automated image collection for 96 hours. The collected images were sorted and further processed with Gimp software.[33] The data evaluation was processed with GraphPad Prism software (GraphPad Software, USA) and log(inhibitor) *vs.* response – variable slope (nonlinear four parameters model) was used to calculate LC50 (50% lethal concentration).[34]

3. Results and discussion

3.1. 3D printing technology and the chip fabrication

For the fabrication of the chip, Digital Light Processing (DLP) 3D printing technology was selected. The main advantage of 3D printing was the possibility to fabricate the whole chip at once, including a complex system of inner channels. Another benefit was the short time (a few hours) needed for fabrication of new products after design changes of the microchannels. Furthermore, less manual work was required to assembly the whole system compared to other available technologies. Although 3D printing is a powerful technology and has a high potential for building millifluidic[32] or microfluidic[30] systems, there are also disadvantages. One of the issues can be the biocompatibility of the printed material.[35] The selected E-Shell 300 resin was recommended for the fabrication of hearing aid shells and otoplasty by the manufacturer because it was CE certified and class-IIa biocompatible according to ISO 10993. However, the toxicity of E-Shell 300 had to be considered.[36–38] Therefore, our 3D printed E-Shell 300 parts were leached in an ethanol bath before use. Another disadvantage of 3D printing can be a low transparency of the printed products.[15] The printing technology is based on stacking the material in layers. Depending on the orientation of the printed parts, an inner microstructure of the surface is created. If the inner and outer surface is not polished, the transparency of the material is limited. Therefore, our produced chips were fabricated as a two-component system in order to preserve the clarity of the bottom layer necessary for the observation of the embryos with an inverted microscope. The body of the chip was 3D printed and the bottom part of the bottom channels was fabricated by lamination of thin, flexible polymeric foil through thin biocompatible lamination adhesive, Fig. 1A.

3.2. Millifluidic chip design optimizations and computer simulations

One of the crucial issues, when designing the geometry of a zebrafish embryo cultivation chip, was to attain accurate displacement and easy manipulation with the embryo in the channels of the chip without any physical damage while keeping the immobilized embryo in the cultivation area. Another issue was to maintain freshness of the cultivation environment (oxygen supply, removal of the developed metabolites *etc.*) by exchange of the cultivation media near the cultivated embryos. There have been microfluidic chips proposed and tested, where one or multiple zebrafish eggs were directly loaded into the cultivation chambers by an operator[20,21,24] and then, the chip was sealed. By using this approach, embryo displacement in the chip was not considered and the microchannels served only for the distribution of the media. Systems, where the media distribution channels were used for loading of the embryos to the chip and where the cultivation chambers at the bottom of the channels served as embryo traps, were also published.[25,26,39] Such chips included suction channels at the

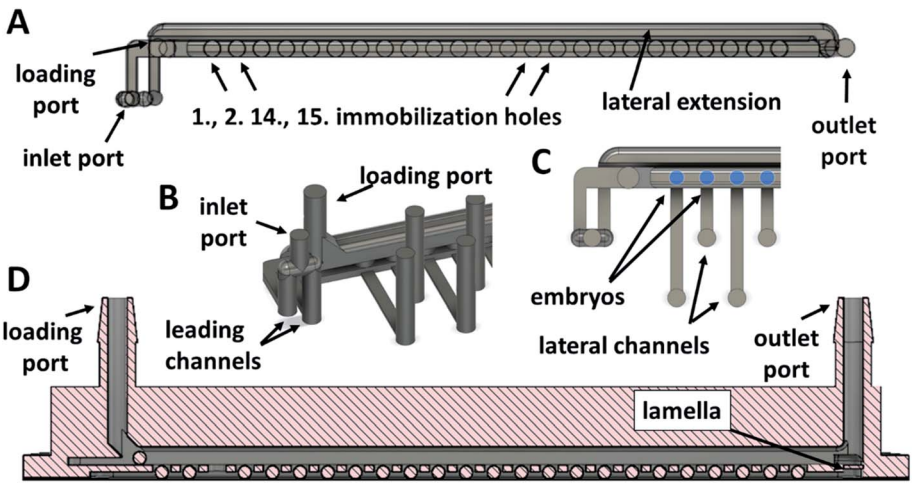

Fig. 2 Details of chip channels. (A) A top view of a fabricated chip with a lateral extension of the bottom channel; (B) a detail of the front part of the chip; (C) a top view of the front part of the chip with immobilized embryos; (D) a side cut view of the whole chip with a lamella on its end.

bottom of the cultivation chambers to retain embryos in the chambers. For increasing the mass transfer of the media around the embryos, modifications of the chamber shapes were proposed.[25] These systems enabled a higher degree of automation of the experiment. Our proposed cultivation chip differs from the published designs by the presence of top and bottom channels separated by a partition with immobilization holes, see Fig. 1D, E, 2A and D. The holes served as cultivation chambers for individual embryos. By such an arrangement of the cultivation chambers, easy manipulation of the embryos in the chip was possible, the embryos were kept in immobilization positions during the media perfusion and a stable mass transfer of the media around the whole surface of all of the cultivated embryos was achieved. Moreover, a facility for individual eggs removal during the cultivation could be added to the current design.

For accurate embryo displacement, the size of the embryo was considered as an important parameter for designing individual chip compartments. Therefore, embryos diameters were examined and variations within the range from ≈900 μm to ≈1300 μm were found, which was comparable to the observations in other studies.[14,20] The following parts of the cultivation system were the most dependent on the diameter of the embryos: (i) the loading and the outlet ports of the chip; (ii) the width and height of the top channel; (iii) the diameter and the depth of the immobilization chambers. Based on numerical simulations and experimental measurements, the following parameters of the chip were used: the width and the height of the top channel and the diameter of the immobilization chambers were all set to 1700 μm, the depth of the immobilization chambers, including the height of the bottom channel and of the partition between the channels, was set to 1250 μm. The size of the bottom channel was adjusted in such a way that the immobilized eggs could not penetrate the space of the lower channel and at the same time, they did not block the newly loaded embryos passing over an already immobilized embryos through the upper channel. The height of the bottom channel of our system was set to 642 μm (including the height of adhesive tape, 142 μm). Details of the designed channels of the chip are presented in Fig. 1K, L, 2 and 3. In Fig. 2A and 3B, a lateral extension of the bottom channel can also be seen on its cross-section, explained further. With the presented microchannel shape and dimensions, no problems with the manipulation of the eggs in the inner space of the final chip design were encountered.

To simplify the chip operation, only one inlet and an outlet port for both channels were used. The inlet port was split into two, leading to the top and to the bottom channels (Fig. 2A and B). Before the outlet port, the channels were merged into one stream. In this rear part of the chip, a lamella was designed (Fig. 2D) to prevent the embryos from falling into the bottom channel and blocking the flow in the bottom channel.

Another requirement was retention of the embryos in their positions in the immobilization chambers during long-term experiments. For this purpose, it was necessary to ensure that the pressure of the liquid in the bottom channel was lower than

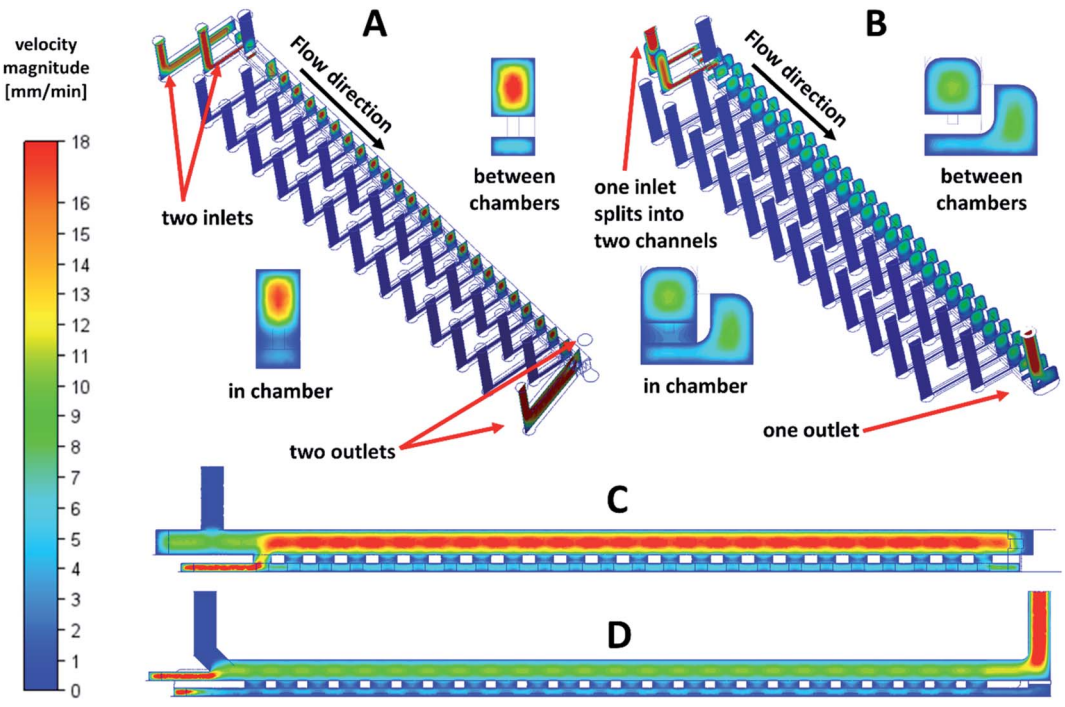

Fig. 3 Numerical simulations of the fluid flow in cultivation chips. (A) The first prototypes of the chip with two independent inlets to the top and to the bottom channel and without a lateral extension of the bottom channel; (B) the final design of the cultivation chamber including a sideway extension of the bottom channel (one chip inlet splits into two channels leading to the top and the bottom channels); (C) a typical velocity magnitude profile in the longitudinal cross-section of the first prototypes of the chip; (D) a typical velocity magnitude profile in the longitudinal cross-section of the final prototypes of the chip. Simulations performed at 30 μl min^{-1}.

or comparable with the pressure in the upper channel. Such pressure distribution prevented the fluid flow from the bottom to the top channel to remove individual embryos from their positions. The ejection of the embryos from the fist immobilization chambers was experimentally observed in the first prototypes of the cultivation chips with two inlets and two outlets. Numerical simulations of the flow velocities in the chip also confirmed (Fig. 3A and B) this phenomenon. The fluid in the bottom channel tended to flow to the top channel through the first immobilization chamber (Fig. 3C). Based on CFD simulations, it was found that to retain the embryos in their positions in the immobilization chambers can be achieved by extending the bottom channel sideways as a lateral extension, Fig. 2A and C. The modelled changes of the design adjustment and velocity field are presented in detail in Fig. 3B and D. In insets (Fig. 3A and B), the parts of the chip in and out of the immobilization chamber are presented. A significant decrease in the flow velocities was observed in the top channel after the optimization of the chip design. The changes in the fluid velocity profile can also be seen in the longitudinal cross-section of the chip (Fig. 3C and D). The observed fluid flow through the first immobilization chamber diminished after the channel shape adjustment. With the change of the bottom channel geometry, loading with 100% efficiency (for detail see Materials and methods) and keeping the embryos in their immobilization positions was performed without any problems.

During perfusion experiments in a cultivation chip, different modes of the media or toxicant flow can usually be applied. It can be *e.g.* a continuous[20,23] or a time-dependent sequential flow[26] of the media or toxicant. Another possibility is a sequential flow switched between a continuous flow of the media and the toxicant,[21] or a looping of the flow[26,39] of the toxicant in the cultivation chamber with its possible regular exchange. The described experimental conditions are connected with the fluid exchange processes in the chip channels and they could also be used to minimize the consumption of the tested chemical species. Moreover, some of them are necessary in experimental setups, when specific developmental stages of fish embryos need to be stimulated. Therefore, to predict and evaluate the fluid exchange process properties (toxicant and nutrition species transport) within the millifluidic chip, other numerical simulations and experimental measurements were performed. Time-lapse images of the simulated two fluids exchange process in the chip with a 150 s time interval for 40 minutes are presented in Fig. 4. The numerical simulations of the fluid exchange process were performed at flow rates of 30 μl min^{-1} and 80 μl min^{-1} (Fig. 4A and D). The relative concentration of the exchanging fluid was expressed by color changes from zero as blue to one as red. Gradual color changes of the fluid concentration were confirmed for both tested flow rates in the whole device. To test the performance of the designed device in experimental conditions, the cultivation chip was filled with the 0.1% solution of trypan blue at the same flow rates, 30 and 80 μl min^{-1} for 40 minutes. Trypan blue solution was considered a fresh fluid exchanging the current fluid in the device channels (Fig. 4B and E). After the channels were filled with the trypan blue solution, the experiment continued for another 40 minutes, and the trypan blue was washed out by E3 media (Fig. 4C and F). The results from the numerical simulations are in good agreement with the

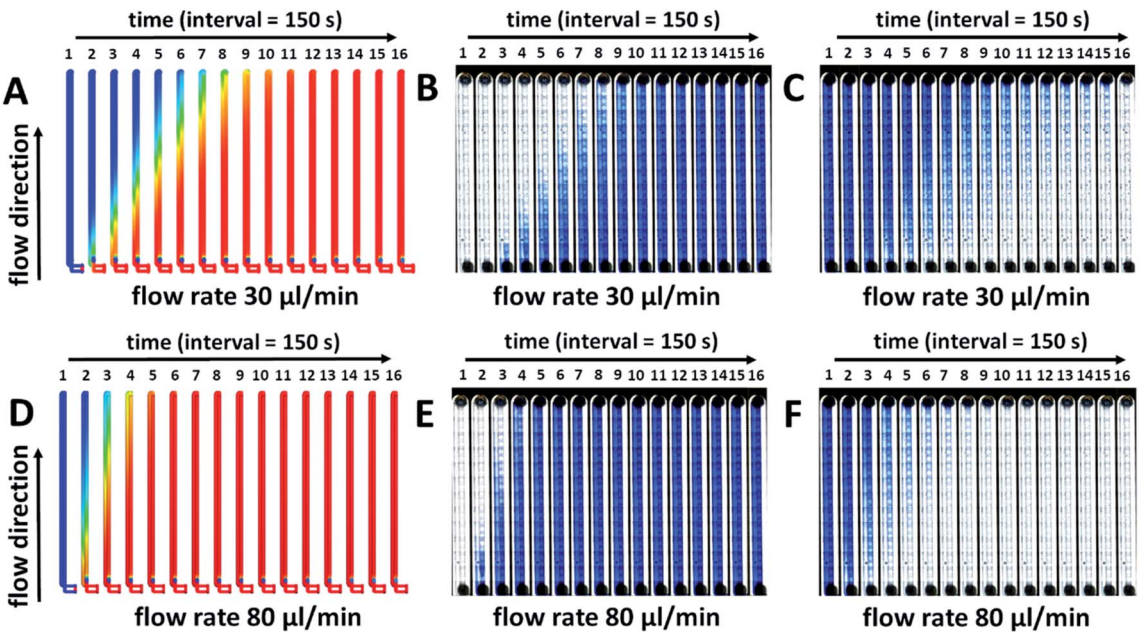

Fig. 4 A numerical simulation and experimental measurements of fluid exchange process through a cultivation chip. The images of the individual vertical channels on each panel represent 150 second time interval of the simulated two fluids exchange process in the chip. (A–C) The fluid exchange process at 30 μl min^{-1}; (D–F) the fluid exchange process at 80 μl min^{-1}; (A and D) a numerical simulation of the exchange process with the relative concentration of exchanging fluid from 0 (blue) to 1 (red); (B and E) the process of filling the channels of the chip with 0.1% solution of trypan blue; (C and F) the process of washing out trypan blue from the channels of the chip.

experimental measurements at the same flow rate. The time intervals of the dye exchange process correspond to the real experiments. The time necessary for a complete exchange of the media in the cultivation chip was ~17–20 min. at a flow rate of 80 μl min^{-1}. (approx. the volume of 1.36–1.60 ml) and 27–30 min. at a flow rate of 30 μl min^{-1}. (approx. the volume of 0.81–0.90 ml). The presented results confirmed the reliability of the fluid exchange process for the given flow rates and were considered for further chip development and experimental setups.

3.3. Embryos removal system

The experimental process of removing individual embryos from a microchannel during cultivation experiments is not usually the aim in long-term cultivation studies due to the need to wait for the embryos to hatch. When it is necessary to collect all the embryos immobilized in wells or chambers and remove them from the cultivation chip, it can usually be done by reversing the flow in the chip.[39] However, it can still be challenging to remove individual embryos, for example, to the observation system of a confocal microscope,[40] or when an unexpected embryo coagulation appears. To unload one or more selected embryos from an immobilization chamber of the chip during or after experiments, a modification of the chip design was proposed. The added functionality of the cultivation chip was fully tested as a proof-of-concept. The adjusted system of the cultivation chip consisted of added lateral channels, which functioned as embryo ejectors (Fig. 1A–C). The mouth of the lateral channels was directed into the bottom part of the bottom cultivation channel in the center of the immobilization chamber. The lateral channels were connected to a 24-port switch valve through an interface module (Fig. 1H, J, 2B, S1B and F†) fixed to the top of the chip. When removal of any of the 24 immobilized embryos was needed, the ejection was performed by switching the valve to the right position and applying the pulse of the flow rate to the selected lateral channel.

The removal process of an immobilized embryo is presented by time-lapse images in Fig. 5A. During the process, the egg was pushed to the side of the immobilization chamber, see Fig. 5A, 1-2. It was lifted and ejected to the top channel (Fig. 5A, 3–5). Then, the egg moved in the direction of the top channel flow (Fig. 5A, 6–8). The lowest flow rate values to eject the embryo to the top channel and to achieve a smooth removal of an egg from an immobilization chamber was set to 80 μl min^{-1} in the chip inlet and 160 μl min^{-1} in the lateral channels. Higher flow rates in the lateral channels resulted in easier embryo ejection. The process was modelled also by numerical simulations. An example of the process simulation is presented in Fig. 5B, where the media flowed through the third (Fig. 5B, 1-2) and through the twenty third (Fig. 5B, 3-4) lateral channel. From analysis of the flow velocity, it can be concluded that the fluid flow directed to a selected chamber in the chip does not increase the flow velocity in the bottom channel in the sense that it does not tend to eject other embryos from the immobilization chamber to the top channel. The process was highly selective for the chosen chamber. This observation was experimentally proved.

To verify the functionality of the embryo removal system, manual and automated Arduino-controlled 24-ports switch valves were proposed. They were fabricated from E-Shell 300 polymer by 3D fabrication technology, see Fig. S1.† The operation of both valves, the manual and the automated, was successfully tested. The 100% functionality of the designed embryo removal system was further confirmed by using 3D printed switch valves. Due to a relatively low long-term working performance of the 3D printed components of the multiport switch valves and a larger complexity of the chip with a removal system (Fig. 1F–J and S1†), the chips were built without lateral channels (Fig. 2A) for long-term cultivation experiments. It was verified by simulations that the fluid flow behavior in the systems without lateral channels is similar to the fluid flow behavior in the chips with a removal system, so the results obtained from the simplified systems could be extrapolated to their more complex counterparts.

3.4. Cultivation experiments and toxicity testing

To achieve an effective embryo manipulation in a chip and an effective distribution of nutrients or toxicants in a chip was the main purpose during the chip design optimization steps and CFD simulations before long-term experiments were performed. The highest fluid velocity was located in the center of

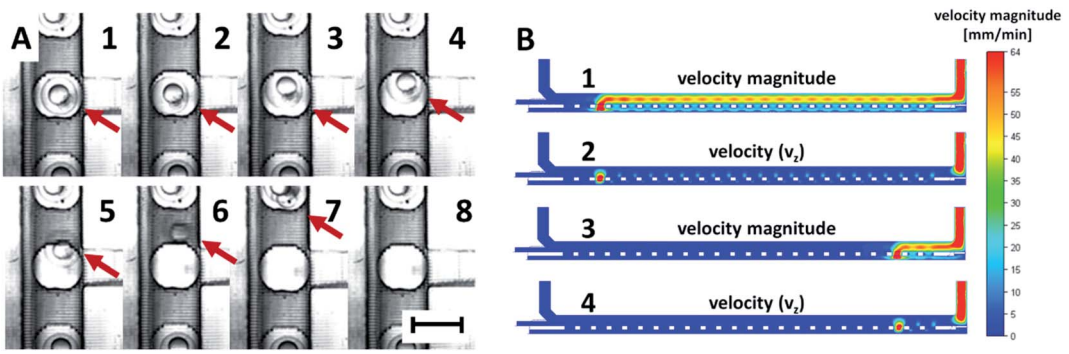

Fig. 5 The function of the embryo removal system. (A1–8) An embryo removal process presented as a time-lapse image recording, the red arrow points to the affected embryo, scale bar: 1.7 mm; (B) A numerical simulation of the flow velocity in the chip (without embryos), where a flow rate of 160 μl min^{-1} was applied to the lateral channel leading to the third (B1-2) and to the twenty-third (B3-4) immobilization chamber.

the top channel and in the center of the lateral extension of the bottom channel (Fig. 5B, insets). It was approximately 4 times higher than in the bottom channel beneath the cultivation chambers. Nevertheless, we supposed it was still sufficient for correct distribution of the media and the oxygen to the whole surface of the immobilized embryos. Based on the CFD simulations, shear stress exerted on the immobilized embryo surface was also evaluated, see details in Fig. 6A. The maximal values of the shear stress magnitude were observed from the top and the lateral sides of the embryos. The observed maxima corresponded to the areas oriented to the top channel and to the lateral extension of the bottom channel (Fig. 6A). The maximum value was 7×10^{-4} Pa at a flow rate 30 μl min^{-1}. This value was lower compared to other studies, where for example, 400 μl min^{-1} flow rate was used with the shear stress in the interval from 1×10^{-2} to 9.8×10^{-2} Pa (ref. 26) or 50 μl min^{-1} with the maximum shear stress 5.2×10^{-3} Pa (ref. 28) with no negative influence of the shear stress on the embryo development. From the given comparisons, it was predicted that the flow rate conditions in our system did not influence a healthy development of zebrafish embryos protected by the chorion. The assumptions stated above were experimentally confirmed by a detailed inspection of the developmental stages of the cultivated embryos under perfusion conditions. The developmental stages of 24 embryos (per experiment) were determined according to Kimmel *et al.*[18] Their representative images are presented in Fig. 6B. The blastula (3 hpf and 4 hpf), the gastrula (6–13 hpf), the segmentation (14–24 hpf), the pharingula (48 hpf) and the hatching (68 hpf) period were observed. The larva at 72 hpf was not present in the chamber of the micrograph because the hatched larvae were no longer immobilized and they moved freely in the chip after the hatching. In these experiments, we achieved 0% mortality at 96 hpf, which was the same as in the control well-based experiments. In both, the perfusion and the well-based experiments, we observed a delay in the embryonic development compared to the well-based tests at 28 °C. The extra time for observation of the developmental stages of zebrafish in the chip was intended as a benefit of the decreased cultivation temperature (25 °C).[21] It was concluded that the set experimental conditions under the perfusion did

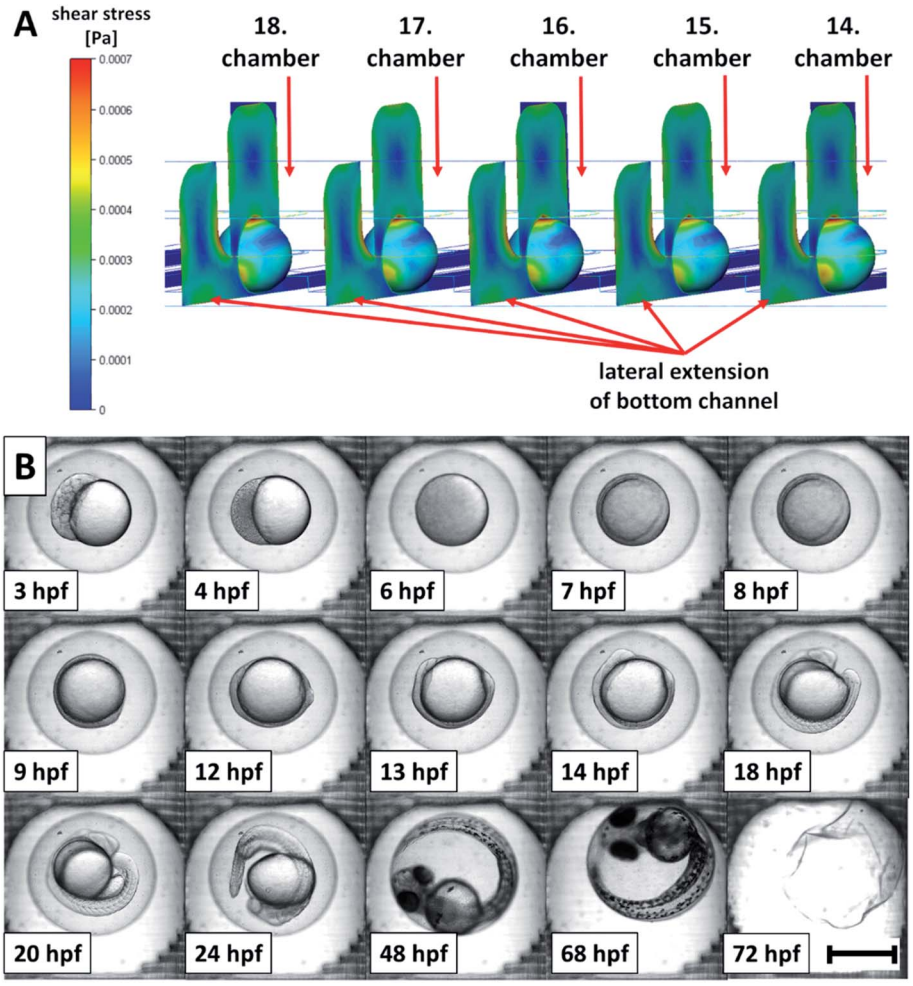

Fig. 6 A numerical simulation of the shear stress and the developmental stages of the embryos. (A) Shear stress exerted on the surface of the embryos in the cultivation chambers (flow rate 30 μl min^{-1}); (B) the developmental stages of a zebrafish embryo during the cultivation experiment over 96 hours, scale bar: 0.6 mm.

not negatively influence the development of the cultivated embryos in the designed chip. This was in agreement with the results in other systems,[21,23] where a normal embryo development was observed in long-term experiments under flow rates in range from 4 μl min^{-1} to 100 μl min^{-1}.

Finally, we evaluated the suitability of the developed perfusion chip for toxicological assays. Ethanol was selected as the model toxic agent because it is a commonly available chemical, it can permeate the embryo through the chorion[31,41,42] and it is a well-known teratogen not only for human but also for zebrafish embryos.[41,43] The ethanol toxicity on the zebrafish development was analyzed in 3D printed chips under perfusion conditions at a constant flow rate of 30 μl min^{-1} of the toxicant and at the same time, in 96-well plates with the standardized FET test. The embryos in the chips were kept under continuous perfusion of ethanol concentrations in E3 media over 96 hours.

The percentage of developmental defects caused by ethanol and expressed as FET test toxicity end-points relative to overall defects observation is presented in Fig. 7A. Pericardial edema was the most frequent morphological marker observed. This observation was in agreement with Reimers *et al.*[43] Embryo coagulation, developmental retardations, and various malformations were observed as well. In FET tests, the number of the observed toxicity end-points was reduced approx. by 10% in comparison with the chips assays. Representative images of the developmental defects are presented in Fig. 7B.

The mortality of the cultivated embryos was evaluated for FET tests (Fig. 7C) and for perfusion assays in the chips (Fig. 7D). A graphical presentation of the mortality showed that the mortality is slightly shifted to lower concentrations of ethanol in the chip assays. This shifting was confirmed by evaluating the median lethal dose (LC50) of ethanol at 72 hpf. It achieved a value of 4.3 g l^{-1} with R^2 0.999 (Goodness of Fit) for the chip assays and 6.3 g l^{-1} with R^2 0.994 (Goodness of Fit) for the FET tests.

In our assays, we observed a higher sensitivity of the embryos to the toxic effect of ethanol in chips compared to *e.g.* the work of Zhu *et al.*[26] and Wielhouwer *et al.*[20] However, we have to be aware of the fact that in the mentioned works, the experimental conditions differed (exposure time, flow rate, temperature, *etc.*).

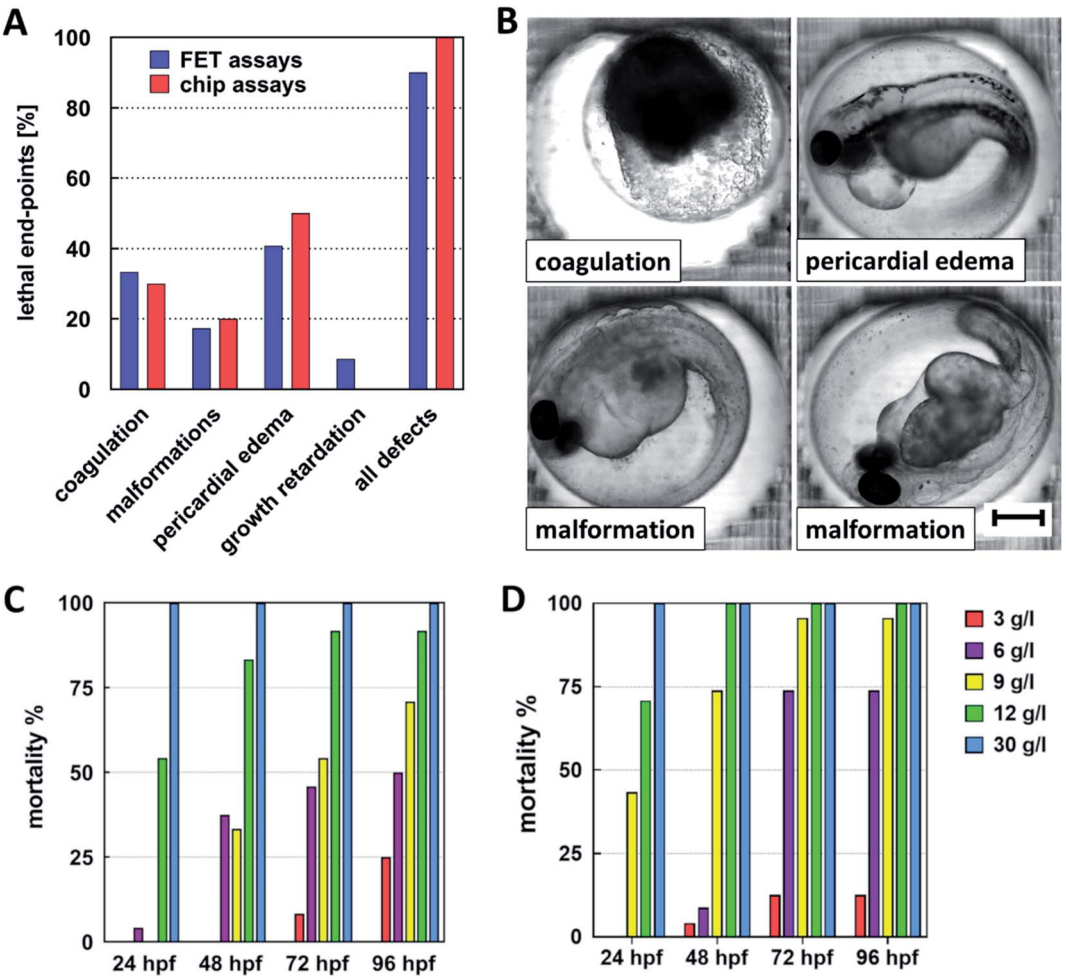

Fig. 7 Developmental defects and mortality of embryos observed in toxicity testing. (A) The percentage of the observed lethal end-points in all toxicological assays; (B) representative micrographs of the selected toxicity end-points presenting coagulation, pericardial edema, and malformations (scale bar: 0.3 mm); zebrafish embryos mortality in an (C) FET test and (D) chip assays. The absence of error bars means a single FET experiment with 24 embryos per concentration as individual replicates.

Nevertheless, the performed perfusion toxicity assays proved that the effect of toxic compounds on the embryonic development of zebrafish can be monitored in the developed chip.

The presented work fills the gap in the recent development of perfusion chip prototypes for zebrafish embryonic assays. Our chip offers an alternative to the other published systems. Technical details of selected published designs and experimental setups are provided in Table 1 in ESI.† In contrast to the published systems, our device design offers improvement in terms of combination of all the demanded properties in one solution. It enables immobilization of multiple embryos in one chip. No fluidic components were designed in the optical path of the camera so it is possible to acquire high quality images. The mass transfer around the cultivated embryos was improved by introducing top and bottom channels and the shear stress acting on the embryos was uniformly distributed in all chambers along the chip. Loading of the embryos to the cultivation chambers could be automated. In order to keep the embryos in the immobilization chambers, no added functionality such as media suction channels under the embryos was required, although the inner volume of the channels slightly increased due to lateral extension of the bottom channel. The proposed removal property can be integrated to the chip and provides not only the collection of all cultivated embryos after the assay but also unloading selected single embryos from the chip during the cultivation if needed.

4. Conclusions

A novel design of zebrafish millifluidic chip for long-term cultivation experiments was proposed, fabricated, and tested. The cultivation chip had one media inlet, one embryo loading inlet, one outlet, and included two channels (a top channel and a bottom channel) in the cultivation area separated by a partition with circular chambers for embryos immobilization. The design of the microchannels in the chip was based on the results of numerical simulations. The chip was developed to load and cultivate 24 embryos in the cultivation chamber. The applied flow rate in the chip provided an exchange of the media near the embryos with acceptable shear stress for their healthy development. Moreover, the numerical simulation showed that the media flows equally around all the embryos along the cultivation system. The design of the chip was also adjusted to provide an individual embryo removal functionality, which has been tested successfully. It can be used during the cultivation experiments for selective unload of any of the cultivated embryos out of the chip. This unique property opens the possibility of detailed studies of selected embryos by additional methods.

DLP 3D printing technology was evaluated for fabrication of the chips. The results have proved that a device with complex channels can be fabricated from E-Shell 300 resin and no toxic effect on the development of the embryos was observed in the chips when the chips were leached in ethanol. For inverted microscopy observation, the low transparency of the cured resin was solved by the fabrication of the device as a two-component system with transparent foil laminated to the bottom part of the chip.

The reliability of the cultivation chip has been verified by long-term perfusion zebrafish cultivation experiments and perfusion tests of toxicity. The cultivation assays run in an automatic manner with an automated image acquisition. All developmental stages of the cultivated embryos could be distinguished with no developmental defects. The toxic effect of ethanol on the embryo development was observed in both the FET tests and the chip assays.

We may conclude that a prototype of a zebrafish cultivation system based on a millifluidic platform fabricated by 3D printing technology has been successfully developed and can be considered for further development of medium-throughput automated systems for both long-term cultivation and for toxicity screening assays.

Conflicts of interest

There are no conflicts to declare.

Acknowledgements

The authors acknowledge the assistance provided by the Research Infrastructure NanoEnviCz (Project No. LM2018124) supported by the Ministry of Education, Youth and Sports of the Czech Republic, the ERDF/ESF project "UniQSurf – Centre of biointerfaces and hybrid functional materials" (No. CZ.02.1.01/0.0/0.0/17_048/0007411), the project No. TJ01000077 of the Technology Agency of the Czech Republic, the project No. UJEP-IGA-TC-2019-53-01-2; UJEP-SGS-2018-53-005-3 and UJEP-SGS-2020-53-006-3.

References

1 OECD, *Test No. 236: Fish Embryo Acute Toxicity (FET) Test*, OECD, 2013.
2 G. J. Lieschke and P. D. Currie, *Nat. Rev. Genet.*, 2007, **8**, 353–367.
3 O. Lohi, M. Parikka and M. Rämet, *Acta Paediatr.*, 2013, **102**, 104–110.
4 J. M. Spitsbergen and M. L. Kent, *Toxicol. Pathol.*, 2003, **31**, 62–87.
5 C. Chakraborty, C. Hsu, Z. Wen, C. Lin and G. Agoramoorthy, *Curr. Drug Metab.*, 2009, **10**, 116–124.
6 L. I. Zon and R. T. Peterson, *Nat. Rev. Drug Discovery*, 2005, **4**, 35–44.
7 K. Bambino and J. Chu, in *Current Topics in Developmental Biology*, Elsevier, 2017, vol. 124, pp. 331–367.
8 *High-throughput Behavioral Screening – ViewPoint*, http://www.viewpoint.fr/en/a/drug-screening, accessed May 4, 2020.
9 E. K. Sackmann, A. L. Fulton and D. J. Beebe, *Nature*, 2014, **507**, 181–189.
10 T. Luo, L. Fan, R. Zhu and D. Sun, *Micromachines*, 2019, **10**, 104.
11 R. C. Lagoy and D. R. Albrecht, *Sci. Rep.*, 2018, **8**, 6217.

12 M. F. Yanik, C. B. Rohde and C. Pardo-Martin, *Annu. Rev. Biomed. Eng.*, 2011, **13**, 185–217.
13 *Life Chip Scientific Equipment Company Ltd.*, http://www.lifechipz.com/, accessed May 4, 2020.
14 F. Yang, C. Gao, P. Wang, G.-J. Zhang and Z. Chen, *Lab Chip*, 2016, **16**, 1106–1125.
15 F. Zhu, J. Skommer, N. P. Macdonald, T. Friedrich, J. Kaslin and D. Wlodkowic, *Biomicrofluidics*, 2015, **9**, 046502.
16 N. M. Fuad, J. Kaslin and D. Wlodkowic, *Biomicrofluidics*, 2017, **11**, 051101.
17 A. Khalili and P. Rezai, *Briefings Funct. Genomics*, 2019, **18**, 419–432.
18 C. B. Kimmel, W. W. Ballard, S. R. Kimmel, B. Ullmann and T. F. Schilling, *Dev. Dyn.*, 1995, **203**, 253–310.
19 E. Lammer, H. G. Kamp, V. Hisgen, M. Koch, D. Reinhard, E. R. Salinas, K. Wendler, S. Zok and Th. Braunbeck, *Toxicol. in Vitro*, 2009, **23**, 1436–1442.
20 E. M. Wielhouwer, S. Ali, A. Al-Afandi, M. T. Blom, M. B. Olde Riekerink, C. Poelma, J. Westerweel, J. Oonk, E. X. Vrouwe, W. Buesink, H. G. J. vanMil, J. Chicken, R. van't Oever and M. K. Richardson, *Lab Chip*, 2011, **11**, 1815.
21 F. Yang, Z. Chen, J. Pan, X. Li, J. Feng and H. Yang, *Biomicrofluidics*, 2011, **5**, 024115.
22 Y. Li, F. Yang, Z. Chen, L. Shi, B. Zhang, J. Pan, X. Li, D. Sun and H. Yang, *PLoS One*, 2014, **9**, e94792.
23 Y. Li, X. Yang, Z. Chen, B. Zhang, J. Pan, X. Li, F. Yang and D. Sun, *Biomicrofluidics*, 2015, **9**, 024105.
24 D. Choudhury, D. van Noort, C. Iliescu, B. Zheng, K.-L. Poon, S. Korzh, V. Korzh and H. Yu, *Lab Chip*, 2012, **12**, 892–900.
25 J. Akagi, K. Khoshmanesh, B. Evans, C. J. Hall, K. E. Crosier, J. M. Cooper, P. S. Crosier and D. Wlodkowic, *PLoS One*, 2012, **7**, e36630.
26 F. Zhu, A. Wigh, T. Friedrich, A. Devaux, S. Bony, D. Nugegoda, J. Kaslin and D. Wlodkowic, *Environ. Sci. Technol.*, 2015, **49**, 14570–14578.
27 H. Becker, *Talanta*, 2002, **56**, 267–287.
28 Z. Zhu, Y. Geng, Z. Yuan, S. Ren, M. Liu, Z. Meng and D. Pan, *Micromachines*, 2019, **10**, 168.
29 F. Zhu, D. Baker, J. Skommer, M. Sewell and D. Wlodkowic, *Cytometry*, 2015, **87**, 446–450.
30 S. Waheed, J. M. Cabot, N. P. Macdonald, T. Lewis, R. M. Guijt, B. Paull and M. C. Breadmore, *Lab Chip*, 2016, **16**, 1993–2013.
31 A. A. Yazdi, A. Popma, W. Wong, T. Nguyen, Y. Pan and J. Xu, *Microfluid. Nanofluid.*, 2016, **20**, 50.
32 M. J. Beauchamp, G. P. Nordin and A. T. Woolley, *Anal. Bioanal. Chem.*, 2017, **409**, 4311–4319.
33 The GIMP Development Team, *GIMP*, 2020.
34 X.-P. Gao, F. Feng, X.-Q. Zhang, X.-X. Liu, Y.-B. Wang, J.-X. She, Z.-H. He and M.-F. He, *Int. J. Toxicol.*, 2014, **33**, 98–105.
35 F. Zhu, T. Friedrich, D. Nugegoda, J. Kaslin and D. Wlodkowic, *Biomicrofluidics*, 2015, **9**, 061103.
36 M. de Almeida Monteiro Melo Ferraz, H. H. W. Henning, P. Ferreira da Costa, J. Malda, S. Le Gac, F. Bray, M. B. M. van Duursen, J. F. Brouwers, C. H. A. van de Lest, I. Bertijn, L. Kraneburg, P. L. A. M. Vos, T. A. E. Stout and B. M. Gadella, *Environ. Sci. Technol. Lett.*, 2018, **5**, 80–85.
37 S. van den Driesche, F. Lucklum, F. Bunge and M. Vellekoop, *Micromachines*, 2018, **9**, 71.
38 Z. Nejedlá, D. Poustka, R. Herma, M. Liegertová, M. Štofik, J. Smejkal, V. Šícha, P. Kaule and J. Malý, *RSC Adv.*, 2021, **11**, 16252–16267.
39 J. Akagi, K. Khoshmanesh, C. J. Hall, J. M. Cooper, K. E. Crosier, P. S. Crosier and D. Wlodkowic, *Sens. Actuators, B*, 2013, **189**, 11–20.
40 T.-Y. Chang, C. Pardo-Martin, A. Allalou, C. Wählby and M. F. Yanik, *Lab Chip*, 2012, **12**, 711–716.
41 S. Ali, D. L. Champagne, A. Alia and M. K. Richardson, *PLoS One*, 2011, **6**, e20037.
42 P. Blader and U. Strähle, *Dev. Biol.*, 1998, **201**, 185–201.
43 M. J. Reimers, A. R. Flockton and R. L. Tanguay, *Neurotoxicol. Teratol.*, 2004, **26**, 769–781.